IEEE Access
Multidisciplinary | Rapid Review | Open Access Journal

Received August 7, 2020, accepted August 17, 2020, date of publication August 20, 2020, date of current version August 28, 2020.

Digital Object Identifier 10.1109/ACCESS.2020.3018195

Radio Vortex Communication System Using Partial Angular Aperture Receiving Scheme Under Atmospheric Turbulence

QIAN MA AND HENG-KAI ZHAO
School of Communication and Information Engineering, Shanghai University, Shanghai 200444, China
Corresponding author: Heng-Kai Zhao (zhaohk@shu.edu.cn)

This work was supported by the National Natural Science Foundation of China under Grant 61871261 and 61271061.

ABSTRACT For transmission based on long-distance vortex waves, the partial receiving scheme which uses a limited angular aperture receiving and demultiplexing multi-beam can solve the difficulty of the conventional whole beam receiving scheme due to the divergence of the vortex beam. But the atmospheric turbulence is rarely considered in analyzing the stability of the radio vortex (RV) communication system based on the partial angular aperture receiving (PAAR) scheme. Here we first introduce atmospheric turbulence into the RV communication system based on the PAAR scheme. Moreover, in order to compare the effects of turbulence on the PAAR scheme and the whole angular aperture receiving (WAAR) scheme, a new turbulence attenuation degree D model is proposed, which represents the stability of the RV communication system in the atmospheric turbulence environment. Simulation results indicate that the difference of D values between PAAR scheme and WAAR scheme does not exceed the order of 0.01 when the range of refractive index structure constant C_n^2 is $10^{-17}m^{-\frac{2}{3}} - 10^{-12}m^{-\frac{2}{3}}$ and the distance is 90m-120m. When the range of C_n^2 is $10^{-13}m^{-\frac{2}{3}} - 10^{-12}m^{-\frac{2}{3}}$ and the distance is 90m-120m, D value of PAAR scheme is always smaller than that of WAAR scheme. These demonstrations suggest that the RV communication system using PAAR scheme is more stable than that using WAAR scheme in the strong atmospheric turbulence environment.

INDEX TERMS Atmospheric turbulence, radio vortex, partial angular aperture receiving scheme.

I. INTRODUCTION

Vortex waves carrying orbital angular momentum (OAM) have infinite orthogonal states in theory, while electromagnetic wave with spin angular momentum (SAM) has only two orthogonal states. Therefore, OAM has attractive potential to significantly increase spectral efficiency and channel capacity for wireless communication [1]. It is verified that OAM multiplexing can achieve great potentials in the radio frequency (RF) wireless communications [2], [3].

We call the wireless communication system based on OAM the radio vortex (RV) communication system. It is well known that the radiation pattern of vortex beams possesses a characteristic [4]: intensity nulls are along the beam axis. Due to the divergence of vortex beams, the further they travel, the larger the radius of the intensity nulls is. Moreover, the larger the OAM mode number l, the more severe the divergence [5]. Hence, a large receiving aperture is required to capture the effective power of the transmitting vortex beams in long distance links. To solve this problem, a partial angular aperture receiving (PAAR) scheme has been proposed [6]. This PAAR scheme can be an effective space-saving and cost-effective method for the RV communication system. It is verified that the orthogonality of Laguerre-Gaussian (LG) eigen beams with different integer topological charges is preserved and independent of the aperture sizes and the radial indices [7]. Therefore, we can still utilize orthogonality of LG eigen beams to increase channel capacity of RV communication system based on PAAR scheme in long distance links.

It is verified that angle and angular momentum are linked by a Fourier transformation [8]. A restriction of the angular range within an optical beam profile generates orbital angular momentum sidebands on the transmitted light and the crosstalk occurs [8]–[10]. In recent years, the relationship between aperture size, OAM mode interval and minimum

The associate editor coordinating the review of this manuscript and approving it for publication was Muhammad Zubair.

crosstalk has been proved by experiments [6], [11]–[15]. These literatures have proved that crosstalk due to limited aperture can be improved by adopting appropriate partial reception scheme. In [15], the influence of additive white Gaussian noise (AWGN) channel on PAAR scheme was analyzed. The influence of AWGN channel and Rician channel on PAAR scheme and the effect of non-ideal receiving condition on partially receiving aperture were also analyzed. However, it does not analyze the influence of atmospheric turbulence channel on the PAAR scheme. Therefore, it is of immediate significance to study the impact of atmospheric turbulence on the RV communication system based on PAAR scheme.

In this paper the impact of atmospheric turbulence on the RV communication system based on PAAR scheme has been investigated. In order to compare the effects of turbulence on PAAR scheme and whole angular aperture receiving (WAAR) scheme, a novel turbulence attenuation D model is proposed. The contributions of this article are summarized as follows:

1) We use a mask model to represent the angular aperture, and then derive the OAM spiral spectrum of the PAAR scheme.

2) According to the channel capacity formula of [16], a channel capacity model of PAAR scheme based on atmospheric turbulence is proposed.

3) A novel turbulence attenuation D model is proposed.

It is necessary to transmit multiple modes simultaneously. However, the number of transmission modes in the scheme of [13] is limited. Therefore, we choose the scheme of [6] to study the influence of atmospheric turbulence on the PAAR scheme. The remainder of this paper is organized as follows. Section II presents the definition of spiral spectrum of the PAAR scheme, capacity model of PAAR scheme based on atmospheric turbulence and turbulence attenuation degree D model. In Section III, the simulation results are analyzed and discussed. Finally, the conclusions are drawn in Section IV.

II. THEORETICAL PRINCIPLE

In order to compare with the WAAR scheme proposed in [17], only the phase distortion of atmospheric turbulence is considered, but the amplitude attenuation caused by atmospheric turbulence is not considered. Fig.1 presents the transmission

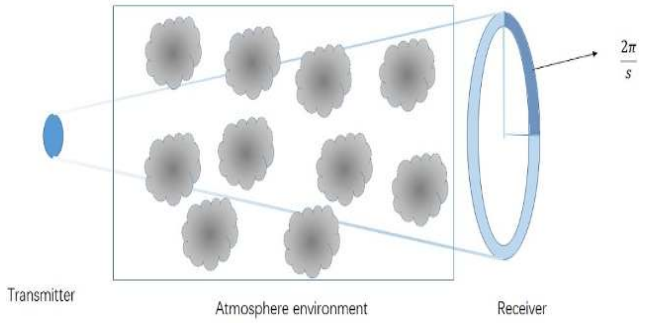

FIGURE 1. RV communication system using a PAAR scheme in the atmospheric turbulent environment.

of RV communication system using a PAAR scheme in the atmospheric turbulent environment. In this paper, we use the WAAR scheme and the PAAR scheme to receive the same OAM state set at the same distance.

A. SPIRAL SPECTRUM OF PAAR SCHEME

The LG beam is used to describe the vortex wave carrying orbital angular momentum. The field distribution of Laguerre-Gauss beam in the source plane ($z = 0$) is expressed as [18]

$$E_{m,n}(r,\phi,0) = \left(\frac{\sqrt{2}r}{w_0}\right)^{m} L_n^m\left(\frac{2r^2}{w_0^2}\right) e^{-im\phi} e^{-\frac{r^2}{w_0^2}} \tag{1}$$

where r is radial distance, ϕ is azimuthal angle, z is propagation distance, i is an imaginary unit, n is the order of the Laguerre polynomial $L_n^m(x)$, $n = 0$ is generally configured for RV systems, $L_n^m(x) = 1$, when $n = 0$. In this paper, we assume that $n = 0$. m is the OAM state, whose absolute value describes the number of twists of the helical wavefront. w_0 is the beam waist radius of LG beam at $z = 0$.

The functional form of the Laguerre-Gauss source mode is well known at any point ($z > 0$) in free space. One has [18]

$$E_{m,n}(r,\phi,z) = \left(\frac{w_0}{w}\right)\left(\frac{\sqrt{2}r}{w}\right)^{m} L_n^m\left(\frac{2r^2}{w^2}\right) \times e^{\{-im\phi - \frac{r^2}{w^2} + i[kz-(m+1)\Phi + \frac{1}{2}\frac{kr^2}{R}]\}}. \tag{2}$$

where $w = w_0\sqrt{1+(\frac{z}{z_R})^2}$, $R = z[1+(\frac{\pi w_0^2}{\lambda z})^2]$, $z_R = \frac{\pi w_0^2}{\lambda}$ is the Rayleigh distance, λ is the wavelength. $\Phi = \arctan(\frac{z}{z_R})$ is the Gouy phase, $k = \frac{2\pi}{\lambda}$ is wave number.

Under the Rytov approximation, when passing through the weak turbulent atmosphere, the beam field received at the receiving aperture at distance z is expressed as [18], [19]

$$\begin{aligned} E_{m,n}^W(r,\phi,z) &= U\left(\frac{r}{R_1}\right)\left(\frac{\sqrt{2}r}{w}\right)^{m}\left(\frac{w_0}{w}\right) L_n^m\left(\frac{2r^2}{w^2}\right) \\ &\quad \times e^{\{-im\phi - \frac{r^2}{w^2} + i[kz-(m+1)\Phi + \frac{kr^2}{2R}] + \psi(r,\phi,z)\}} \\ &= U\left(\frac{r}{R_1}\right) E_{m,n}(r,\phi,z) e^{\psi(r,\phi,z)}. \end{aligned} \tag{3a}$$

where $U(\frac{r}{R_1}) = \begin{cases} 1 & 0 < \frac{r}{R_1} \le 1 \\ 0 & \frac{r}{R_1} > 1 \end{cases}$, R_1 is the receiving aperture radius. In this paper, we know $U(\frac{r}{R_1}) = 1$. $\psi(r,\phi,z)$ is the phase distortion term caused by the atmospheric turbulence. Based on the quadratic approximation [20], $\psi(r,\phi,z)$ satisfies

$$e^{(\psi(r,\phi,z)+\psi^*(r,\phi',z))} = e^{\frac{2r^2}{r_0^2}(cos(\phi'-\phi)-1)}. \tag{3b}$$

where r_0 is the spatial coherence radius of the LG beam under the Kolmogorov turbulence flow model. r_0 is expressed as [20]

$$r_0 = \left[\frac{8}{3(\alpha + 0.618\Lambda^{\frac{11}{6}})}\right]^{\frac{3}{5}} (1.46C_n^2k^2z)^{-\frac{3}{5}}. \tag{4a}$$

with

$$\alpha = \frac{1-\Theta^{\frac{8}{3}}}{1-\Theta}. \tag{4b}$$

$$\Lambda = \frac{2z}{kw^2}. \tag{4c}$$

where $\Theta = 1 + \frac{z}{R}$ is the curvature parameter of the LG beam at receiver, Λ is the Fresnel ratio of the LG beam at receiver, C_n^2 is the refractive index structure constant. The larger C_n^2 is, the greater the turbulence strength is [16].

It is well known that the radius of the OAM annular region with the maximum energy strength is denoted by [21]

$$r_{\max}(z) = \sqrt{\frac{|m|}{2}} w(z). \tag{5}$$

$r_{\max}(z)$ determines the size of the receiving aperture. Only when the receiving aperture is larger than $r_{\max}(z)$, can the complete energy of the beam be received.

For the PAAR scheme, the receiver should be placed at the maximum beam strength, therefore the integral range of the receiving radius of the PAAR scheme is (r_1, r_2). For the WAAR scheme, the receiver is placed at the center of the beam, therefore the integral range of the WAAR scheme is $(0, R_1)$. In this article $r_2 \leq R_1$.

The aperture is considered a mask [10]. For the WAAR scheme without angle limitation, the mask is

$$M(\phi) = 1, 0 < \phi \leq 2\pi. \tag{6}$$

For the WAAR scheme without angle limitation, the received field can be described as $E_{m,n}^W(r, \phi, z)M(\phi)$.

For the PAAR scheme with angle limitation, the mask is

$$M'(\phi) = \begin{cases} 1, & 0 < \phi \leq \dfrac{2\pi}{s} \\ 0, & \dfrac{2\pi}{s} < \phi \leq 2\pi \end{cases}. \tag{7}$$

For the PAAR scheme, since the receiver uses an angular aperture of $\frac{2\pi}{s}$, the received field can be described as $E_{m,n}^W(r, \phi, z)M'(\phi)$. It can be seen that the partial aperture receiving field is $\frac{1}{s}$ of the whole aperture receiving field.

For the WAAR scheme, according to the reference [22], the field distribution of Eq. (3a) is expanded according to the spiral spectrum harmonics. Therefore, Eq. (3a) can be written as

$$\begin{aligned} E_{m,n}^W(r, \phi, z) &= E_{m,n}(r, \phi, z)e^{\psi(r,\phi,z)} \\ &= \frac{1}{\sqrt{2\pi}} \sum_{l=-\infty}^{\infty} \alpha_l^{WAAR}(r, z)e^{-il\phi}. \end{aligned} \tag{8a}$$

with

$$\alpha_l^{WAAR}(r, z) = \frac{1}{\sqrt{2\pi}} \int_0^{2\pi} E_{m,n}^W(r, \phi, z)e^{il\phi} d\phi. \tag{8b}$$

It is well known that the energy of the beam is $E = 2\varepsilon_0 \sum_{l=-\infty}^{\infty} C_l^{WAAR}$, $C_l^{WAAR} = \int_0^{R_1} \left|\alpha_l^{WAAR}(r, z)\right|^2 rdr$. ε_0 is permittivity of vacuum.

If the field received by the whole aperture is $E_{m,n}^W(r, \phi, z)$, then the field received by the partial aperture is

$$\begin{aligned} E_{m,n}^P(r, \phi, z) &= U(\frac{r}{R_1})E_{m,n}(r, \phi, z)e^{\psi(r,\phi,z)} \\ &= \frac{1}{s} E_{m,n}^W(r, \phi, z). \end{aligned} \tag{9a}$$

Therefore, Eq.(9a) can be written as

$$E_{m,n}^P(r, \phi, z) = \frac{1}{\sqrt{2\pi}} \sum_{l=-\infty}^{\infty} \alpha_l^{PAAR}(r, z)e^{-il\phi}. \tag{9b}$$

with

$$\alpha_l^{PAAR}(r, z) = \frac{1}{\sqrt{2\pi}} \int_0^{2\pi} E_{m,n}^P(r, \phi, z)e^{il\phi} d\phi. \tag{9c}$$

In the PAAR scheme, the spiral spectrum with OAM state l is expressed as

$$P_l^{PAAR}(m, z) = \frac{C_l^{PAAR}(m, z)}{\sum_{q=-\infty}^{\infty} C_q^{PAAR}(m, z)}. \tag{10}$$

In the PAAR scheme, we can derive the spiral spectrum with OAM state l (details are in Appendix) as

$$\begin{aligned} P_l^{PAAR}(m, z) &= \frac{C_l^{PAAR}}{C_{initial}} \\ &= \frac{1}{s^2} \frac{\int_0^{R_1} \frac{w_0^2}{w^2} (\frac{2r^2}{w^2})^m e^{-2r^2(\frac{1}{w^2}+\frac{1}{r_0^2})} I_{l-m}(\frac{2r^2}{r_0^2}) rdr}{\int_0^{R_1} (\frac{2r^2}{w_0^2})^m e^{\frac{-2r^2}{w_0^2}} rdr}. \end{aligned} \tag{11}$$

B. CAPACITY MODEL OF PAAR SCHEME BASED ON ATMOSPHERIC TURBULENT

In the absence of atmospheric turbulence, the capacity of the RV communication system using WAAR scheme on the AWGN channel is expressed as [16]:

$$\begin{aligned} C_{ideal} &= \frac{L}{2} erfc(\sqrt{\frac{P_{TX}}{2N_0}}) log_2(\frac{1}{2} erfc(\sqrt{\frac{P_{TX}}{2N_0}})) + L \\ &\quad + (L - \frac{L}{2} erfc(\sqrt{\frac{P_{TX}}{2N_0}})) log_2(1 - \frac{1}{2} erfc(\sqrt{\frac{P_{TX}}{2N_0}})). \end{aligned} \tag{12}$$

where L is the number of channels. N_0 is the additive white Gaussian noise power, P_{TX} is the transmitted power. $erfc(.)$ is the complementary error function.

In the literature [15], [23], the theoretical perfect demodulation performance is independent of the aperture size in the AWGN channel. That is to say, the WAAR scheme has the same capacity as the PAAR scheme when there are the same number of OAM states in the AWGN channel. Next we

derive the channel capacity in the presence of atmospheric turbulence.

In PAAR scheme, in order to transmit multiple mutually orthogonal OAM modes simultaneously at the same frequency, it is necessary to select a specific OAM modal set. It can be known from the literature [6] that the OAM state set must satisfy

$$l_k = l_1 + ks. \tag{13}$$

The OAM state set transmitted by the transmitter is assumed as B. In order to better compare the performance of WAAR and PAAR scheme in atmospheric turbulence environments, the transmission mode set of WAAR scheme is the same as that of PAAR scheme. Under the influence of turbulence, the OAM multiplexing beam will deviate from the center of the beam, causing crosstalk between adjacent modes [24]. We choose $L = 2k+1$ symmetrically distributed channels, $B = \{l_1 - ks, \ldots, l_1, \ldots, l_1 + ks\}$. Therefore, the crosstalk matrix of RV system with PAAR scheme can be expressed as Eq.(14), shown at the bottom of the next page. where $P^{PAAR}_{l_1-qs}(l_1 - ps, z)$, $-k \le p \le k$, $-k \le q \le k$ is the power weight of the spiral harmonic component with OAM state $l_1 - qs$, when the vortex wave with the OAM state $l_1 - ps$ is transmitted in atmosphere environments. When $p \ne q$, $P^{PAAR}_{l_1-qs}(l_1 - ps, z)$ represents that the normalized wave power is spread from the state $l_1 - ps$ into the state $l_1 - qs$. The p-th row of matrix P^{PAAR} indicates that the normalized wave power of the p-th channel is spread into the vortex channels which are included in the entire set B. The q-th column of the matrix P^{PAAR} includes the desired wave power of q-th vortex channel and the spread wave power from other vortex channels which are included in the set B. Therefore, an expression of the signal-to-interference-and-noise ratio (SINR)can be obtained from each column of crosstalk matrix P^{PAAR} of RV system based on PAAR scheme. The expression is

$$\gamma^{PAAR} = \left[\gamma^{PAAR}_{-k} \ \ldots \ \gamma^{PAAR}_{q} \ \ldots \ \gamma^{PAAR}_{k}\right]. \tag{15a}$$

with

$$\gamma^{PAAR}_{q} = \frac{P^{PAAR}_{l_1-qs}(l_1 - qs, z)}{\sum\limits_{p\in B}^{p\ne q} P^{PAAR}_{l_1-qs}(l_1 - ps, z) + \frac{N_0}{P_{TX}}} \tag{15b}$$

where γ^{PAAR}_{q} is the SINR of the q-th OAM state. When the RV communication systems apply the Quadrature Phase Shift Keying (QPSK) modulation, the bit error rate of OAM channels is derived as

$$p^{PAAR} = \left[p^{PAAR}_{-k} \ \ldots \ p^{PAAR}_{q} \ \ldots \ p^{PAAR}_{k}\right]. \tag{16a}$$

with [25]

$$p^{PAAR}_{q} = \frac{1}{2} erfc\left(\sqrt{\frac{\gamma^{PAAR}_{q}}{2}}\right). \tag{16b}$$

where p^{PAAR}_{q} is the bit error rate of the q-th OAM state. According to the bit error rate, the capacity of the q-th vortex channel can be expressed as

$$C(p^{PAAR}_{q}) = 1 + \mathrm{p}^{PAAR}_{q}\log_2(\mathrm{p}^{PAAR}_{q}) + (1 - \mathrm{p}^{PAAR}_{q})log_2(1 - \mathrm{p}^{PAAR}_{q}). \tag{17a}$$

with

$$C^{PAAR}_{L} = \left[C(p^{PAAR}_{-k}) \ \ldots \ C(p^{PAAR}_{q}) \ \ldots \ C(p^{PAAR}_{k})\right] \tag{17b}$$

Therefore, the capacity of the RV communication system based on atmospheric turbulence is

$$C^{PAAR} = \sum_{q\in B} C(p^{PAAR}_{q}). \tag{18}$$

which is the row sum of the capacity matrix C^{PAAR}_{L} in Eq.(17b).

C. TURBULENCE ATTENUATION DEGREE MODEL

We express the channel capacity of the WAAR scheme proposed in [17] as C^{WAAR}. In order to compare the turbulence effects on the WAAR scheme and the PAAR scheme, a novel turbulence attenuation degree D model is proposed, which represents the stability of the RV communication system in the atmospheric turbulence environment. The absolute value of channel capacity difference between the RV communication system in turbulent environment ($C_n^2 = 0.5 \times 10^{-17}m^{-\frac{2}{3}} - 0.5 \times 10^{-11}m^{-\frac{2}{3}}$) and the RV communication system in weak turbulence environment ($C_n^2 = 0.5 \times 10^{-17}m^{-\frac{2}{3}}$) is defined as the numerator of turbulence attenuation degree D. The channel capacity of the RV communication system in the weak turbulent environment ($C_n^2 = 0.5 \times 10^{-17}m^{-\frac{2}{3}}$) is defined as the denominator of turbulence attenuation degree D. The channel capacity of RV communication system (including WAAR scheme and PAAR scheme) is C

$$C = \sum_{\mathrm{q}\in B} C(p_q). \tag{19}$$

If the refractive index structure constant C_n^2 is given, the spatial coherence radius of the LG beam under the C_n^2 can be expressed as $r_0(C_n^2)$, substituting C_n^2 in Eq.(4a). The channel capacity of RV communication system in the weak turbulent environment ($C_n^2 = 0.5 \times 10^{-17}m^{-\frac{2}{3}}$) is $C_{C_n^2=0.5\times10^{-17}}$. We use the spatial coherence radius of the LG beam at the $C_n^2 = 0.5 \times 10^{-17}m^{-\frac{2}{3}}$ and the channel capacity of RV communication system in Eq.(19), to express $C_{C_n^2=0.5\times10^{-17}}$

$$C_{C_n^2=0.5\times10^{-17}} = C(r_0(C_n^2 = 0.5 \times 10^{-17}m^{-\frac{2}{3}})). \tag{20a}$$

The channel capacity of the RV communication system in the turbulent environment is $C_{C_n^2}$,

$$C_{C_n^2} = C(r_0(C_n^2)). \tag{20b}$$

where $0.5 \times 10^{-17}m^{-\frac{2}{3}} \le C_n^2 \le 0.5 \times 10^{-11}m^{-\frac{2}{3}}$.

Hence, the expression of turbulence attenuation degree D is

$$D = \frac{\left| C_{C_n^2} - C_{C_n^2=0.5\times10^{-17}} \right|}{C_{C_n^2=0.5\times10^{-17}}}. \tag{21}$$

The larger the value of D, the greater the influence of turbulence.

III. SIMULATION RESULTS AND DISCUSSIONS

Generally speaking, the mode selection of vortex beam in PAAR scheme is limited by different factors, including receiver aperture size and circular arc s. Given a fixed receiver aperture size, a larger OAM mode value may result in a larger beam size at the receiver, which may decrease the recovered power. Hence, special attention should be paid to the selection of OAM mode set. In this section, a partial aperture receiving scheme in the atmospheric turbulent environment is simulated. We set the propagation distance to 100m. In [26], vortex phase properties of OAM keep well after long-distance transmission, which were experimentally demonstrated. Hence, as long as the OAM receiving antenna is improved and the OAM modes of PAAR scheme satisfies Eq.(13), it can provide ideal orthogonality for a set of regular OAM modes after long-distance transmission. The system simulation parameter settings are shown in Table 1.

TABLE 1. RV system simulation parameters.

simulation parameter	value
beam waist radius w_0	0.01m
propagation distance z	100m
transmission frequency f	100GHz
refractive index structure constant C_n^2	$1.0\times10^{-12}m^{-\frac{2}{3}}$
signal-to-noise ratio SNR	10dB
radius of receiver R_1	50m
circular arc s	4

In the absence of atmospheric turbulence, the transmission channel is a Gaussian channel, which is considered to be an ideal situation. Fig.2(a) shows the channel capacity comparison between the PAAR scheme ($s = 2, 4$) and the WAAR scheme ($s = 1$) under ideal conditions. We can observe that the PAAR scheme has the same capacity as the WAAR scheme when the transmission distance achieves 100 meters. This is because of the fact that theoretical perfect demodulation performance is independent of the aperture size. Fig.2(b) shows the channel capacity comparison between the PAAR scheme ($s = 2, 4$) and the WAAR scheme ($s = 1$) under a non-ideal condition where the transmission environment is the presence of atmospheric turbulence. We choose the refractive index structure constant $C_n^2 = 1.0 \times 10^{-12}m^{-\frac{2}{3}}$ as the non-ideal condition. With an identical number of OAM states, the WAAR scheme has more capacity than the PAAR scheme when the transmission distance achieves 100 meters. For instance, when the L is 13, the capacity of $s = 1$ in the WAAR scheme is 4.062 bits/L-channels, while that of $s = 2(s = 4)$ in the PAAR scheme is 2.8 bits/L-channels (1.251 bits/L-channels). When the transmission distance achieves over 100 meters, the PAAR scheme still has the same capacity as the WAAR scheme under ideal conditions and the WAAR scheme still has more capacity than the PAAR scheme under a non-ideal condition.

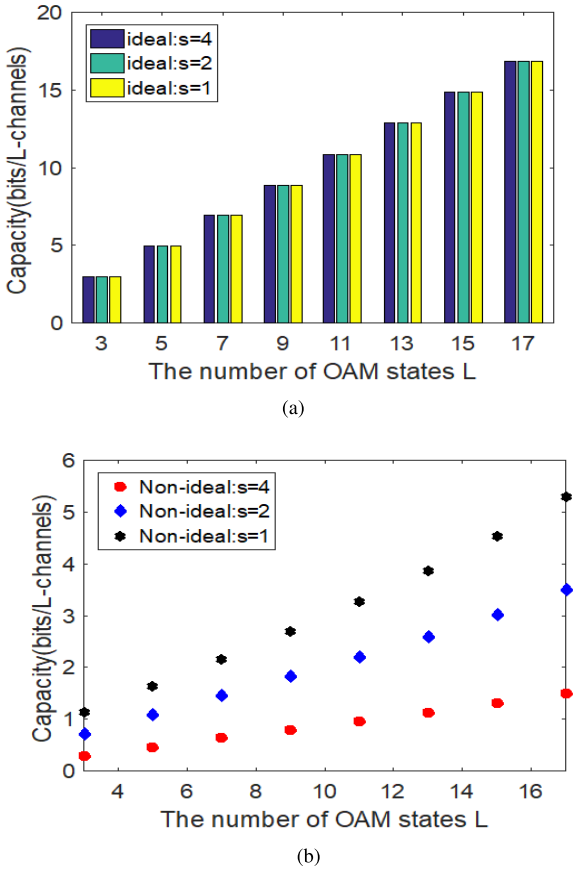

FIGURE 2. The channel capacity comparisons (a) under ideal conditions,(b)under non-ideal conditions.

$$P^{PAAR} = \begin{bmatrix} P^{PAAR}_{l_1-ks}(l_1-ks,z) & \dots & P^{PAAR}_{l_1-qs}(l_1-ks,z) & \dots & P^{PAAR}_{l_1+ks}(l_1-ks,z) \\ \dots & \dots & \dots & \dots & \dots \\ P^{PAAR}_{l_1-ks}(l_1-ps,z) & \dots & P^{PAAR}_{l_1-qs}(l_1-ps,z) & \dots & P^{PAAR}_{l_1+ks}(l_1-ps,z) \\ \dots & \dots & \dots & \dots & \dots \\ P^{PAAR}_{l_1-ks}(l_1+ks,z) & \dots & P^{PAAR}_{l_1-qs}(l_1+ks,z) & \dots & P^{PAAR}_{l_1+ks}(l_1+ks,z) \end{bmatrix}. \tag{14}$$

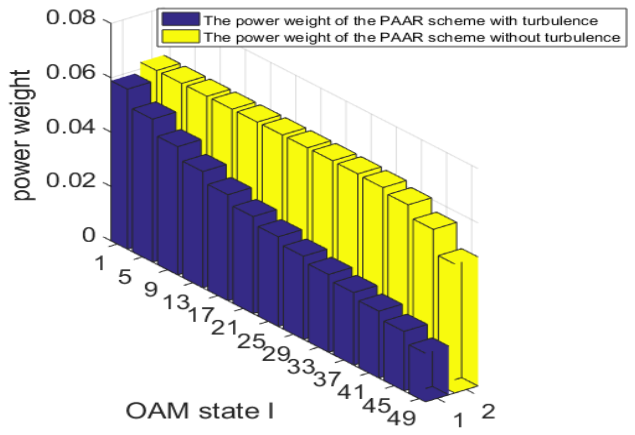

FIGURE 3. The effect of turbulence ($C_n^2 = 1.0 \times 10^{-12} m^{-\frac{2}{3}}$) on the power weight of the PAAR scheme.

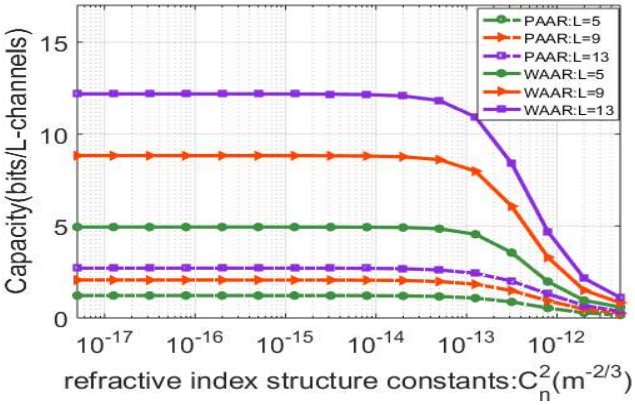

FIGURE 4. simulated capacity curves of L channels.

Fig.3 depicts the effect of turbulence ($C_n^2 = 1.0 \times 10^{-12} m^{-\frac{2}{3}}$) on the power weight of the PAAR scheme. It is verified that the presence of atmospheric turbulence causes crosstalk between OAM states. We see that the power weight of the PAAR scheme with turbulence decreases with the increase of l. The power weight of the PAAR scheme without turbulence initially maintains a fixed value of 0.0625. When l increases to 33, the power weight of the PAAR scheme without turbulence decreases with the increase of l, mainly because of the divergence caused by excessive OAM state l. We also observe that in the case of the identical OAM state, the PAAR scheme with turbulence has much less power weight than PAAR scheme without turbulence. Taking $l = 13$ as an example, the power weight of the PAAR scheme without turbulence is 0.0625, and the power weight with turbulence is 0.0428.

The capacity of RV communication system using PAAR scheme (s=4) and RV communication system using WAAR scheme are depicted as functions of C_n^2 in Fig.4. The typical value of C_n^2 is in the range of $10^{-17} m^{-\frac{2}{3}} - 10^{-12} m^{-\frac{2}{3}}$. It can be seen from the Fig.4 that in the case of the weak and medium turbulent environment, the channel capacity of the PAAR scheme ($L = 5, 9, 13$) and the WAAR scheme ($L = 5, 9, 13$) are fixed. However, when C_n^2 is $1.256 \times 10^{-13} m^{-\frac{2}{3}}$, the channel capacity of the PAAR scheme and the WAAR scheme decrease rapidly with the increase of C_n^2. With an identical L, the PAAR scheme has much less capacity than the WAAR scheme when the C_n^2 increases. For example, when the C_n^2 is $3.155 \times 10^{-13} m^{-\frac{2}{3}}$, the capacity of 5 vortex channels in the WAAR scheme is 3.553 bits/L-channels, while the capacity of 5 vortex channels in the PAAR scheme is 0.8743 bits/L-channels.

In order to determine the practical feasibility of PAAR scheme, we need to study from the turbulence attenuation degree D. The turbulence attenuation degree D based on PAAR scheme ($L = 5, 9, 13$) and based on WAAR scheme ($L = 5, 9, 13$) are simulated as functions of refractive index structure constant C_n^2 (see Fig.5(a)). We see that the turbulence attenuation degree D values of PAAR scheme are nearly same as that of WAAR scheme at different distances, suggesting that PAAR scheme can be used in the practical RV wireless communication system transmission. We see that D values of the PAAR scheme and WAAR scheme increase rapidly with the increase of C_n^2. We also observe that the difference of the turbulence attenuation degree D values between PAAR scheme and WAAR scheme does not exceed the order of 0.01 with C_n^2 of the range of $10^{-17} m^{-\frac{2}{3}} - 10^{-12} m^{-\frac{2}{3}}$. For example, when C_n^2 is $1.991 \times 10^{-12} m^{-\frac{2}{3}}$, $z = 100m$, the turbulence attenuation degree D in the PAAR scheme (in the WAAR scheme) is 0.7874 (0.8225). The turbulence attenuation degree D values based on PAAR scheme ($L = 5, 9, 13$) and based on WAAR scheme ($L = 5, 9, 13$) are depicted as functions of distance in Fig.5(b). We see that in the case of the weak and medium turbulent environment ($10^{-17} m^{-\frac{2}{3}} - 10^{-14} m^{-\frac{2}{3}}$), the turbulence attenuation degree D values in the PAAR scheme are always larger than that the WAAR scheme (except $L = 5$) with identical distance. We also observe that in the case of the strong turbulent environment ($C_n^2 = 1.0 \times 10^{-12} m^{-\frac{2}{3}}$), the turbulence attenuation degree D values in the PAAR scheme are always less than that the WAAR scheme with identical distance. D values of the PAAR scheme and WAAR scheme increase rapidly with the increase of distance. The turbulence attenuation degree D curves of WAAR scheme rise in a broken line because of the limitation of the receiving aperture.

Fig.6 depicts the influence of signal-to-noise ratio(SNR) on the capacity of RV communication system using PAAR scheme ($L = 5, 9, 17$) and RV communication system using WAAR scheme ($L = 5, 9, 17$) in turbulent environment. With an identical L, the channel capacity of the PAAR scheme and the WAAR scheme increase with the increase of SNR. When SNR is less than 36dB, the WAAR scheme has more capacity than the PAAR scheme. With the increase of SNR, the PAAR scheme achieves the same capacity as the WAAR scheme. This is because with the increase of SNR, the crosstalk caused by turbulence is negligible.

Fig.7(a) shows the effect of atmospheric turbulent refractive index constant C_n^2 and SNR on the turbulence attenuation

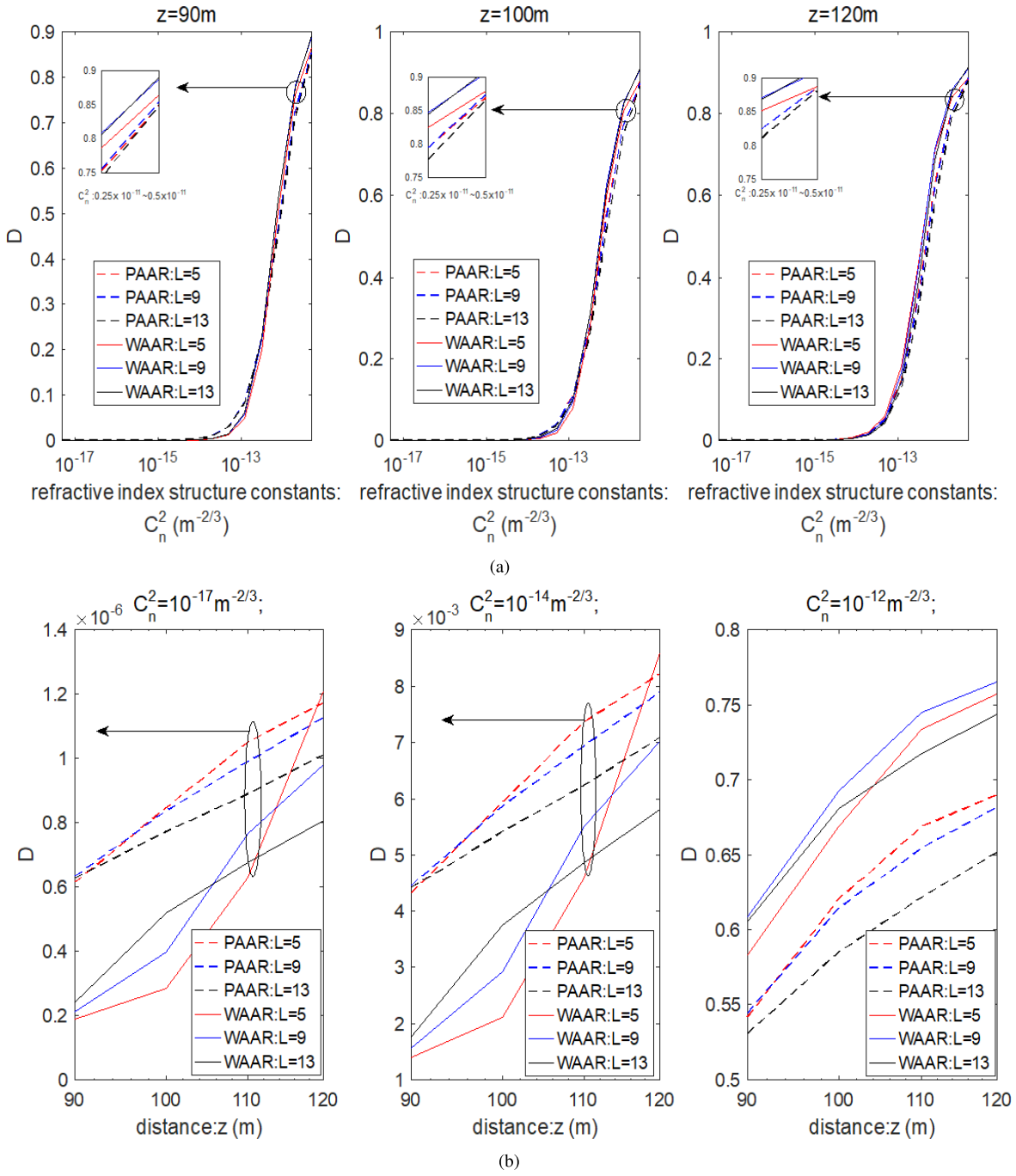

FIGURE 5. The turbulence attenuation degree D based on PAAR scheme ($L = 5, 9, 13$) and based on WAAR scheme ($L = 5, 9, 13$) are simulated as functions (a) of refractive index structure constant C_n^2 with identical distances, (b) of distance with identical refractive index structure constant C_n^2.

degree D of the PAAR scheme. Fig.7(b) depicts the effect of atmospheric turbulent refractive index constant C_n^2 and SNR on the turbulence attenuation degree D of the WAAR scheme. We can observe that the value of the turbulence attenuation degree D is very small in the weak and medium turbulence environment and the turbulence attenuation degree D increases with the increase of C_n^2 in the strong turbulence environment (Fig.7 (a), Fig.7 (b)). We also observe that the turbulence attenuation degree D of the PAAR scheme increases first and then decreases with the increase of SNR (Fig.7 (a), Fig.7 (b)). This means that there is the value of SNR that maximizes the value of turbulence attenuation degree D. We define the turbulence attenuation degree D, which represents the stability of the

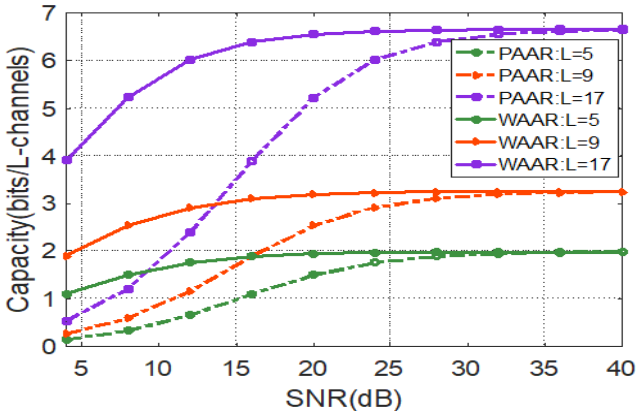

FIGURE 6. The effect of SNR on the RV communication system capacity.

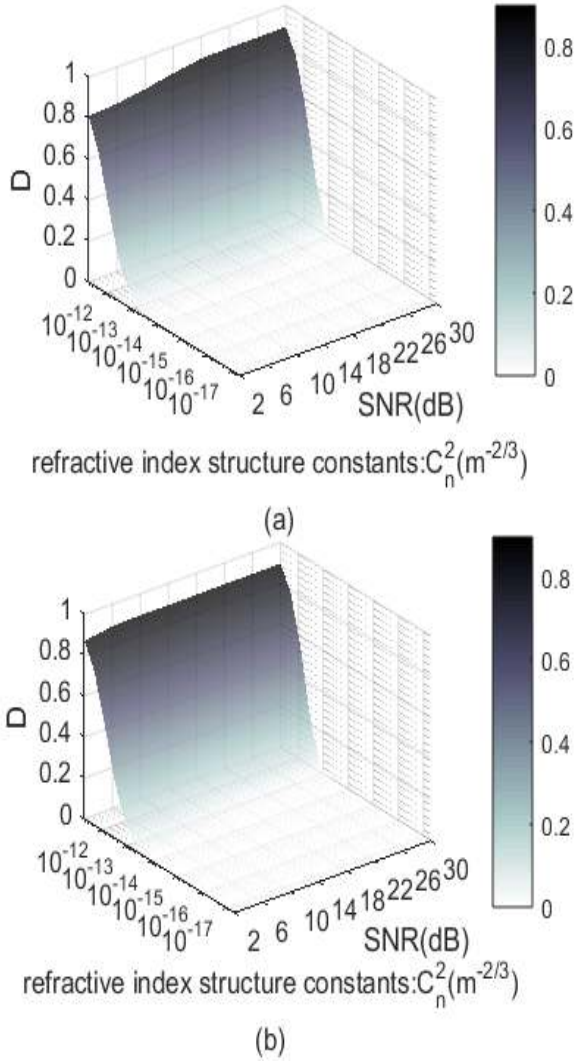

FIGURE 7. The effect of atmospheric turbulent refractive index constant C_n^2 and SNR on (a) the RV communication system capacity using the PAAR scheme, (b) the RV communication system capacity using the WAAR scheme.

RV communication system in the atmospheric turbulence environment. We know that the greater the value of turbulence attenuation degree D, the greater the turbulence impact on the RV communication system. In order to ensure the stability of RV communication system, this SNR should be avoided. Compared with. Fig.7 (a) and Fig.7(b), we find that the turbulence attenuation degree D of PAAR scheme is always smaller than that of WAAR scheme under the same conditions. It is confirmed that in the same strong turbulence environment, the RV communication system using PAAR scheme is more stable than that using WAAR scheme.

IV. CONCLUSION

In this article, the influence of atmospheric turbulence on the stability of RV communication system based on PAAR scheme is investigated. The spiral spectrum of PAAR scheme is first derived. Then the capacity model of PAAR scheme based on atmospheric turbulent is presented. Finally, we propose the turbulence attenuation degree D, which represents the stability of the RV communication system in the atmospheric turbulence environment. Theoretical analysis and numerical results are presented. First, the analysis and numerical results show that in the case of high SNR, RV communication system based on PAAR scheme has a large channel capacity. Second, the turbulence attenuation degree D of RV communication system using PAAR scheme is studied. By comparing the turbulence attenuation degree D of RV communication system using PAAR scheme with that of RV communication system using WAAR scheme, it is found that the difference of the turbulence attenuation degree D values between PAAR scheme and WAAR scheme does not exceed the order of 0.01 with C_n^2 of the range of $10^{-17}m^{-\frac{2}{3}} - 10^{-12}m^{-\frac{2}{3}}$. Consequently, we prove that the RV communication system using PAAR scheme is more stable than that using WAAR scheme in the strong atmospheric turbulence environment. When the range of C_n^2 is $10^{-13}m^{-\frac{2}{3}} - 10^{-12}m^{-\frac{2}{3}}$ and the distance is 90m-120m, D values of PAAR scheme is always smaller than that of WAAR scheme.

To summarize, we can draw a conclusion in this article that from the perspective of turbulence attenuation degree D, the partial aperture receiving scheme can replace the whole aperture receiving scheme in the environment of strong turbulence. All the results in this article are based on the assumption that only the phase distortion of atmospheric turbulence is considered, but the amplitude attenuation caused by atmospheric turbulence is not considered. If we consider the amplitude attenuation caused by atmospheric turbulence, what will happen remains to be further studied, but we believe that even if we consider the amplitude attenuation caused by atmospheric turbulence, the PAAR scheme can provide an opportunity for RV communication system to increase the transmission distance.

APPENDIX

In this appendix, $C_l^{PAAR}(m, z)$ and C_{initial} are derived.

The $\left|\alpha_l^{PAAR}(r,z)\right|^2$ obtained according to the definition of the spiral spectrum is

$$\begin{aligned}
&\left|\alpha_l^{PAAR}(r,z)\right|^2 \\
&= \frac{1}{2\pi}\int_0^{2\pi}\int_0^{2\pi} E_{m,n}^{P}(r,\phi,z)e^{il\phi}E_{m,n}^{P*}(r,\phi',z)e^{-il\phi'}d\phi d\phi' \\
&= \frac{1}{2\pi}\int_0^{2\pi}\int_0^{2\pi} \frac{1}{s}E_{m,n}(r,\phi,z)e^{\psi(r,\phi,z)}\frac{1}{s}E_{m,n}^{*}(r,\phi',z)e^{\psi^*(r,\phi',z)} \\
&\quad\times e^{il(\phi-\phi')}d\phi d\phi' \\
&= \frac{1}{2\pi s^2}\int_0^{2\pi}\int_0^{2\pi} E_{m,n}(r,\phi,z)E_{m,n}^{*}(r,\phi',z)e^{\frac{2r^2}{r_0^2}(cos(\phi'-\phi)-1)} \\
&\quad\times e^{il(\phi-\phi')}d\phi d\phi' \\
&= \frac{1}{2\pi s^2}\frac{w_0^2}{w^2}\left(\frac{2r^2}{w^2}\right)^m e^{-2r^2\left(\frac{1}{w^2}+\frac{1}{r_0^2}\right)}\int_0^{2\pi}\int_0^{2\pi} e^{i(m-l)(\phi'-\phi)} \\
&\quad\times e^{\frac{2r^2}{r_0^2}(cos(\phi'-\phi))}d\phi d\phi' \\
&= \frac{2\pi}{s^2}\frac{w_0^2}{w^2}\left(\frac{2r^2}{w^2}\right)^m e^{-2r^2\left(\frac{1}{w^2}+\frac{1}{r_0^2}\right)} I_{l-m}\left(\frac{2r^2}{r_0^2}\right). \qquad (22)
\end{aligned}$$

where $\int_0^{2\pi} e^{[-im\phi+\eta cos(\phi-\phi')]}d\phi = 2\pi e^{-im\phi'}I_m(\eta)$ [27], $I_m(.)$ is the modified m-order Bessel function of the first kind, R_1 is the radius of receiver.

Hence, $C_l^{PAAR}(m,z)$ is expressed by

$$C_l^{PAAR}(m,z) = \int_0^{R_1}\frac{2\pi}{s^2}\frac{w_0^2}{w^2}\left(\frac{2r^2}{w^2}\right)^m e^{-2r^2\left(\frac{1}{w^2}+\frac{1}{r_0^2}\right)} \times I_{l-m}\left(\frac{2r^2}{r_0^2}\right)rdr. \qquad (23)$$

The electric field of (1) at $z=0$ is expressed as

$$E_{m,n}(r,\phi,0) = \frac{1}{\sqrt{2\pi}}\beta_m(r,0)e^{-im\phi}. \qquad (24a)$$

with

$$|\beta_m(r,0)|^2 = 2\pi\left(\frac{2r^2}{{w_0}^2}\right)^m e^{\frac{-2r^2}{w_0^2}}. \qquad (24b)$$

When $z=0$, $\sum_{q=-\infty}^{\infty} C_q^{PAAR}(m,z)$ is denoted as the $C_{initial}$ and $C_{initial}$ is expressed by

$$\begin{aligned}
C_{\text{initial}} &= \int_0^{R_1}|\beta_m(r,0)|^2 rdr \\
&= \int_0^{R_1} 2\pi\left(\frac{2r^2}{{w_0}^2}\right)^m e^{\frac{-2r^2}{w_0^2}} rdr. \qquad (25)
\end{aligned}$$

REFERENCES

[1] J. Wang, J.-Y. Yang, I. M. Fazal, N. Ahmed, Y. Yan, H. Huang, Y. Ren, Y. Yue, S. Dolinar, M. Tur, and A. E. Willner, "Terabit free-space data transmission employing orbital angular momentum multiplexing," *Nature Photon.*, vol. 6, no. 7, pp. 488–496, Jun. 2012.

[2] F. Tamburini, E. Mari, A. Sponselli, B. Thidé, A. Bianchini, and F. Romanato, "Encoding many channels on the same frequency through radio vorticity: First experimental test," *New J. Phys.*, vol. 14, no. 3, Mar. 2012, Art. no. 033001.

[3] Y. Yan, G. Xie, M. P. J. Lavery, H. Huang, N. Ahmed, C. Bao, Y. Ren, Y. Cao, L. Li, Z. Zhao, A. F. Molisch, M. Tur, M. J. Padgett, and A. E. Willner, "High-capacity millimetre-wave communications with orbital angular momentum multiplexing," *Nature Commun.*, vol. 5, no. 1, p. 4876, Sep. 2014.

[4] T. Yuan, H. Wang, Y. Qin, and Y. Cheng, "Electromagnetic vortex imaging using uniform concentric circular arrays," *IEEE Antennas Wireless Propag. Lett.*, vol. 15, pp. 1024–1027, 2016.

[5] M. J. Padgett, F. M. Miatto, M. P. J. Lavery, A. Zeilinger, and R. W. Boyd, "Divergence of an orbital-angular-momentum-carrying beam upon propagation," *New J. Phys.*, vol. 17, no. 2, Feb. 2015, Art. no. 023011.

[6] S. Zheng, X. Hui, J. Zhu, H. Chi, X. Jin, S. Yu, and X. Zhang, "Orbital angular momentum mode-demultiplexing scheme with partial angular receiving aperture," *Opt. Express*, vol. 23, no. 9, p. 12251, Apr. 2015.

[7] X. Zhong, Y. Zhao, G. Ren, S. He, and Z. Wu, "Influence of finite apertures on orthogonality and completeness of laguerre-Gaussian beams," *IEEE Access*, vol. 6, pp. 8742–8754, 2018.

[8] A. K. Jha, B. Jack, E. Yao, J. Leach, R. W. Boyd, G. S. Buller, S. M. Barnett, S. Franke-Arnold, and M. J. Padgett, "Fourier relationship between the angle and angular momentum of entangled photons," *Phys. Rev. A, Gen. Phys.*, vol. 78, no. 4, Oct. 2008, Art. no. 043810.

[9] S. Franke-Arnold, S. M. Barnett, E. Yao, J. Leach, J. Courtial, and M. Padgett, "Uncertainty principle for angular position and angular momentum," *New J. Phys.*, vol. 6, no. 1, p. 103, 2004.

[10] B. Jack, M. J. Padgett, and S. Franke-Arnold, "Angular diffraction," *New J. Phys.*, vol. 10, no. 10, pp. 6456–6460, Oct. 2008.

[11] G. Xie, Y. Ren, H. Huang, Y. Yan, C. Bao, N. Ahmed, M. Willner, M. P. J. Lavery, M. J. Padgett, and A. E. Willner, "Analysis of aperture size for partially receiving and de-multiplexing 100-Gbit/s optical orbital angular momentum channels over free-space link," in *Proc. IEEE Globecom Workshops (GC Wkshps)*, Atlanta, GA, USA, Dec. 2013, pp. 1116–1120.

[12] G. Xie, Y. Ren, H. Huang, N. Ahmed, L. Li, Y. Yan, M. P. Lavery, M. Padgett, M. Tur, S. Dolinar, and A. Willner, "Experimental comparison of single and double partial receiver apertures for recovering signals transmitted using orbital-angular-momentum," in *Proc. CLEO*, San Jose, CA, USA, 2014, Paper. SM3J-2.

[13] Y. Hu, S. Zheng, X. Jin, X. Zhang, Z. Zhang, and H. Chi, "Simulation of orbital angular momentum radio communication systems based on partial aperture sampling receiving scheme," *IET Microw., Antennas Propag.*, vol. 10, no. 10, pp. 1043–1047, Jul. 2016.

[14] C. J. Vourch, B. Allen, and T. D. Drysdale, "Planar millimetre-wave antenna simultaneously producing four orbital angular momentum modes and associated multi-element receiver array," *IET Microw., Antennas Propag.*, vol. 10, no. 14, pp. 1492–1499, Nov. 2016.

[15] Y. Hu, "Research on new technology of vortex electromagnetic wave receiving," M.S. thesis, Dept. Electron. Eng., Zhejiang Univ., Zhejiang, China, 2016.

[16] J. A. Anguita, M. A. Neifeld, and B. V. Vasic, "Turbulence-induced channel crosstalk in an orbital angular momentum-multiplexed free-space optical link," *Appl. Opt.*, vol. 47, no. 13, pp. 2414–2429, May 2008.

[17] H. Lou, X. Ge, and Q. Li, "The new purity and capacity models for the OAM-mmWave communication systems under atmospheric turbulence," *IEEE Access*, vol. 7, pp. 129988–129996, 2019.

[18] Y. Zhang, M. Tang, and C. Tao, "Partially coherent vortex beams propagation in a turbulent atmosphere," *Chin. Opt. Lett.*, vol. 3, no. 10, pp. 559–561, Oct. 2005.

[19] C. Paterson, "Atmospheric turbulence and orbital angular momentum of single photons for optical communication," *Phys. Rev. Lett.*, vol. 94, no. 15, Apr. 2005, Art. no. 153901.

[20] L.C. Andrews and R.L. Phillips, *Laser Beam Propagation Through Random Media*, 2nd ed., Bellingham, WA, USA: SPIE Press, 2005.
[21] L. Wang, X. Ge, R. Zi, and C.-X. Wang, "Capacity analysis of orbital angular momentum wireless channels," *IEEE Access*, vol. 5, pp. 23069–23077, 2017.
[22] L. Torner, J. P. Torres, and S. Carrasco, "Digital spiral imaging," *Opt. Express*, vol. 13, no. 3, pp. 873–881, Feb. 2005.
[23] H. Jing, W. Cheng, X.-G. Xia, and H. Zhang, "Orbital-Angular-Momentum versus MIMO: Orthogonality, degree of freedom, and capacity," in *Proc. IEEE 29th Annu. Int. Symp. Pers., Indoor Mobile Radio Commun. (PIMRC)*, Bologna, Italy, Sep. 2018, pp. 1–7.
[24] M. Malik, M. O'Sullivan, B. Rodenburg, M. Mirhosseini, J. Leach, M. P. J. Lavery, M. J. Padgett, and R. W. Boyd, "Influence of atmospheric turbulence on optical communications using orbital angular momentum for encoding," *Opt. Express*, vol. 20, no. 12, pp. 13195–13200, Jun. 2012.
[25] Y. Feng and Y. Guo, *Principles of Communication System*. Beijing, China: Tsinghua Univ. Press, 2011.
[26] Y. Yao, X. Liang, W. Zhu, J. Geng, and R. Jin, "Experiments of orbital angular momentum phase properties for long-distance transmission," *IEEE Access*, vol. 7, pp. 62689–62694, 2019.
[27] I. S. Gradshteyn and I. M. Ryzhik, *Table of Integrals, Series, and Products*, 6th ed., New York, NY, USA: Academic, 2000.

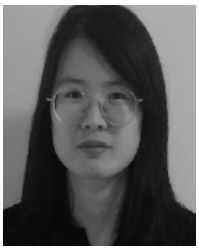

QIAN MA received the B.S. degree in electronic Information engineering from Hebei Normal University, Hebei, China, in 2018. She is currently pursuing the M.S. degree in communication and information system with the School of Communication and Information Engineering, Shanghai University. Her research interests include radio vortex wave propagation in atmospheric turbulence.

HENG-KAI ZHAO received the B.S. and M.S. degrees in electronic instruments and measurement technology from the Shanghai University of Science and Technology, in 1990, and the Ph.D. degree in communication and information systems from Shanghai University, China, in 2006. He is currently an Associate Professor with the School of Communication and Information Engineering, Shanghai University. His research interests include rail transit wireless communications, and radio wave propagation in atmospheric turbulence and signal detection.